

Extended Fractal Fits to Riemann Zeros

Paul B. Slater*

ISBER, University of California,

Santa Barbara, CA 93106

(Dated: February 8, 2022)

Abstract

We extend to the first 300 Riemann zeros, the form of analysis reported by us in *Canad. J. Phys.* **85**, 1 (2007) (also arXiv:math-ph/0606005), in which the largest study had involved the first 75 zeros. Again, we model the nonsmooth fluctuating part of the Wu-Sprung potential, which reproduces the Riemann zeros, by the alternating-sign sine series fractal of Berry and Lewis $A(x, \gamma)$. Setting the fractal dimension equal to $\frac{3}{2}$, we estimate the frequency parameter (γ), plus an overall scaling parameter (σ) introduced. We search for that pair of parameters (γ, σ) which *minimizes* the least-squares fit of the lowest 300 eigenvalues — obtained by solving the one-dimensional stationary (non-fractal) Schrödinger equation with the trial potential (smooth *plus* nonsmooth parts) — to the first 300 Riemann zeros. We randomly sample values within the rectangle $0 < \sigma < 3, 0 < \gamma < 25$. The fits obtained are compared to those gotten by using simply the *smooth* part of the Wu-Sprung potential *without* any fractal supplementation. Some limited improvement is again found. There are two (primary and secondary) quite distinct subdomains, in which the values giving improvements in fit are concentrated.

PACS numbers: Valid PACS 02.10.De, 03.65.Sq, 05.45.Df, 05.45.Mt

Keywords: Riemann zeros, Wu-Sprung potential, Berry-Lewis alternating-sign sine series fractal, Schrödinger equation, fractal potential, affine scaling law, deterministic Weierstrass-Mandelbrot fractal function

*Electronic address: slater@kitp.ucsb.edu

I. INTRODUCTION

Our objective here is the discernment of structural patterns within the nontrivial Riemann zeros (that is, the real parts $\alpha_k > 0$ of the zeros of the Riemann zeta function $\zeta(s)$, which conjecturally all take the form $\frac{1}{2} + \alpha_k i$). More specifically, following our work in [1] (also arXiv:math-ph/0606005), we seek to model the fractal component of the potential which reproduces the α_k 's. The (dominant) smooth part of such a potential can be written implicitly in the form,

$$x_{WS}(V) = \frac{1}{\pi} \left(\sqrt{V - V_0} \ln \frac{V_0}{2\pi e^2} + \sqrt{V} \ln \frac{\sqrt{V} + \sqrt{V - V_0}}{\sqrt{V} - \sqrt{V - V_0}} \right). \quad (1)$$

(Here $V_0 = 3.10073\pi \approx 9.74123$.) This formula (1) was derived by Wu and Sprung [2] by solving a form of Abel's integral equation obtained by the application of the semiclassical approximation to the formula,

$$N(E) = \frac{E}{2\pi} \ln \frac{E}{2\pi E} + \frac{7}{8}, \quad (2)$$

for the smooth part of the number of Riemann zeros less than E (cf. [3]).

In [1], we modeled the fractal component by the alternating-sign sine series fractal (a particular case of a deterministic Weierstrass-Mandelbrot fractal function) of Berry and Lewis [4, eq. (5)],

$$A(x, \gamma) = \sum_{m=-\infty}^{\infty} \frac{(-1)^m \sin \gamma^m x}{\gamma^{(2-d)m}}, \quad (1 < d < 2, 1 < \gamma). \quad (3)$$

Here, d is the fractal dimension, which — following the box-counting argument of Wu and Sprung [2] (cf. [5]) — we took to be $\frac{3}{2}$. (van Zyl and Hutchinson also came to the same conclusion regarding the fractal dimension, independently of which of two distinct inversion techniques they employed [5].) We have, in this $d = \frac{3}{2}$ Berry-Lewis context, a specific case,

$$A(\gamma x, \gamma) = -\gamma^{\frac{1}{2}} A(x, \gamma), \quad (4)$$

of the “affine scaling law” [4, eq. (3)].

In the most extensive of the three ($n = 25, 50, 75$) analyses reported in [1], we found that values of the frequency parameter γ in the vicinity of 3 (and, secondarily, 9) tended to provide the best fits to the Riemann zeros (α_k 's) themselves [1, Fig. 16]. (The sum of the inverted Wu-Sprung potential (1) plus the alternating-sign sine series (3), with γ fixed at

various random values, was used in these analyses as an adjusted potential, which served as input to the time-independent one-dimensional Schrödinger equation. The eigenvalues obtained are, then, regarded as fits to the corresponding Riemann zeros.)

Here, we continue along these same investigative lines, quadrupling the sample size of zeros from 75 to 300. We achieve this substantial increase mainly through reducing — from 5,625 to 600 — the basis size employed in the Arnoldi method for finding eigenvalues of sparse matrices as well as sampling 6,500 points, not 10,000, in the Mathematica program supplied to us by M. Trott. (We also truncate the series (3) at $m = 40$, while in [1] we used a cutoff of $m = 30$ — which, of course, does not reduce computational time.) Despite these reductions, our program, when we employ just the smooth (unsupplemented) Wu-Sprung potential (1), yielded what we deemed to be a suitably acceptable prediction of 542.023 for the (highest) 300-*th* Riemann zero, that is, 541.847. (It would certainly be of interest to evaluate the sensitivity of our results to the various computer program parameters employed and adjust them accordingly, but it would seem to be overwhelmingly time-consuming to do so in substantial detail. We also tried to adopt our Mathematica program to analyze the first 500 Riemann zeros, but we could not adjust the parameters to provide us with an acceptable fit, as measured by comparing the 500-*th* eigenvalue with the 500-*th* Riemann zero.)

While, in the $n = 75$ analysis in [1], we randomly sampled values of $\gamma \in [0, 10]$, here we expand the interval to $\gamma \in [0, 25]$, and as in the first of the analyses ($n = 25$) in [1], allow the series (3) to be scaled by an overall factor of σ , we take now to lie in the interval $[0, 3]$. (We arrived at this rectangular range of parameters from which to extensively sample, after a number of preliminary analyses.)

In Fig. 1 we show the results obtained by randomly sampling points in the indicated base two-dimensional rectangle and determining how well the so-supplemented smooth Wu-Sprung potential fits the first 300 Riemann zeros. Only those 213 points (of the 3,330 sampled) for which the fit is improved for all three measures $S_k(\sigma, \gamma) = \sum_{k=1}^{300} |\tilde{\alpha}_k - \alpha_k|^j$, $j = 1, \frac{3}{2}, 2$ are displayed. (The $\tilde{\alpha}_k$'s denote, say, the eigenvalues, and the α_k 's the Riemann zeros.) These measures were, respectively, 116.265, 86.3596 and 68.1307 when no fractal component was added, and only the smooth potential employed. So, Fig. 1 contains only points for which all three indicators are less than these three values. All the improvements are rather minor in character — as in [1] — with none exceeding one-percent in terms of the

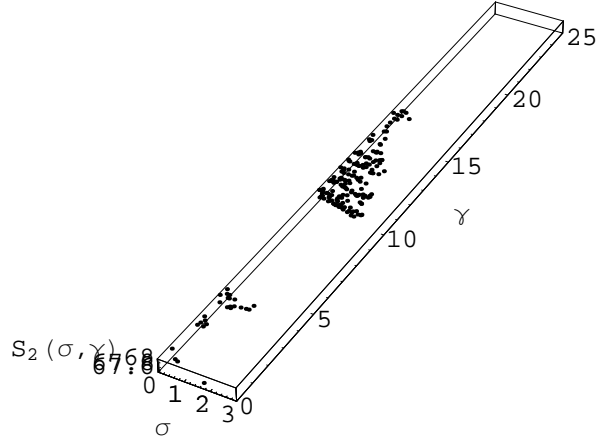


FIG. 1: Those 100 pairs (σ, γ) which give improved alternating-sign sine series (3) fits (for all $k = 1, \frac{3}{2}, 2$) to the first 300 Riemann zeros. 20,000 pairs were randomly, *uniformly* sampled over the base rectangle ($0 < \sigma < 3, 0 < \gamma < 25$). The third axis $S_2(\sigma, \gamma)$ gives the associated least-square fit ($j = 2$) — smaller values, of course, denoting better fits to the zeros. The minimum value of 67.562 is attained at (10.4444, 1.50996).

criterion values $S_k(\sigma, \gamma)$. We observe that for most of these points yielding improvements in fit, we have $\gamma > 10$, a region that was outside the range of consideration in [1]. The minimum values using the $j = 1$ and $j = \frac{3}{2}$ criteria, 115.451 and 85.6691, were attained at the same point $\gamma = 10.3954, \sigma = 1.55535$, while using the $j = 2$ (least-squares) criterion, the minimizing point, with the value 67.562, was located at $\gamma = 10.4444, \sigma = 1.50996$. (For all of the 213 improving values, we had $\sigma < 1.85799$.)

In Figs. 2 and 3, we magnify the regions in Fig. 1, in which the improvements in fit are concentrated.

We also investigated the possibility of modifying our analyses by adding a prefactor of $\gamma^{-\frac{\sigma}{2}}$ to (3) to enhance periodicity, following certain suggestions of Tricot [6, sec. 12.11], but this led to convergence problems, which we did not know immediately how to overcome. Of course, it would be of interest to employ still other basic (few-parameter) fractal models in addition to (3) in similar analyses of the fractal component of the Wu-Sprung potential for the Riemann zeros, possibly thereby achieving greater improvements in fits to the zeros than

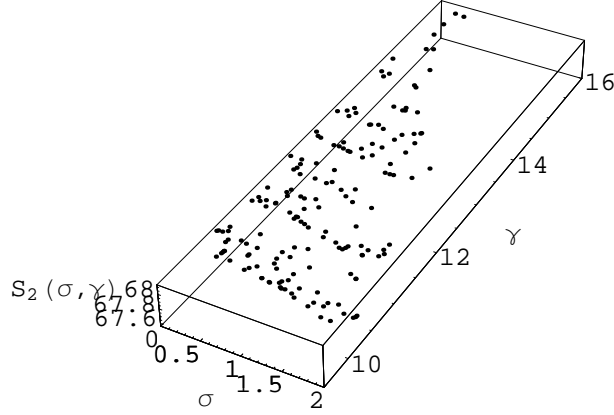


FIG. 2: Magnification of primary domain of fit-improving points in Fig. 1

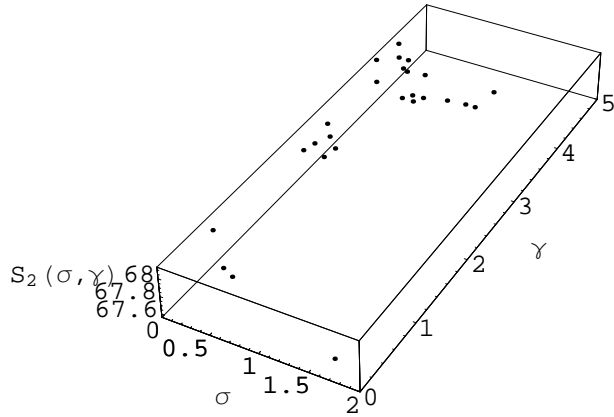


FIG. 3: Magnification of secondary domain of fit-improving points in Fig. 1

we have so far been able to obtain. (In this regard, the companion cosine series of Berry and Lewis [4, eq. (4)] is of potential interest, although unlike (3), it is never negative, so it would seem necessary to add some negative quantity to it.)

It would also be of interest to directly model the fractal component remaining when the smooth Wu-Sprung potential is fitted to the Riemann zeros (cf. [2, inset, Fig. 2] [5, Fig. 3 (a)-(c)]), rather than having — as we have done here and in [1] — inputting each candidate for the fractal component into the time-independent one-dimensional Schrödinger equation.

Acknowledgments

I would like to express gratitude to the Kavli Institute for Theoretical Physics (KITP) for computational support in this research.

- [1] P. B. Slater, *Canad. J. Phys.* **85** (5), 1 (2007).
- [2] H. Wu and D. W. L. Sprung, *Phys. Rev. E* **48**, 2595 (1993).
- [3] N. García, *The one dimensional approachissimo quantum harmonic oscillator: The Hilbert-Polya Hamiltonian for the primes and the zeros of the Riemann function*, quant-ph/0611134.
- [4] M. V. Berry and Z. V. Lewis, *Proc. Roy. Soc. London A* **370**, 459 (1980).
- [5] B. P. van Zyl and D. A. W. Hutchinson, *Phys. Rev. E* **67**, 066211 (2003).
- [6] C. Tricot, *Curves and Fractal Dimensions* (Springer-Verlag, New York, 1995).